# Application of CCD Technology to Produce Imagery from Radar Data

W. E. Arens*
*Jet Propulsion Laboratory, California Institute of Technology, Pasadena, Calif.*

**A real-time aircraft synthetic-aperture radar (SAR) image processor using charge-coupled device (CCD) technology has been developed. Both range and azimuth convolution are accomplished using CCD transversal filtering in the analog domain. The computational equivalency of a CCD transversal filter to comparatively more complex digital processing implementations provides significant reductions in processor power, weight, size, and cost requirements. This paper describes the results of the aircraft CCD SAR image-processor development work to date.**

## I. Introduction

RADAR imaging using side-looking synthetic-aperture radar (SAR) techniques is the best known approach for achieving high-resolution imagery through planetary atmospheric cloud cover. However, if the radar echo data are not processed into images onboard the spacecraft or aircraft, very large quantities of raw uncorrelated data must be sent to Earth for processing. Conversely, if images are produced onboard in real time, multiple-look data may be superimposed into single frames and conventional data-compression algorithms may be applied to significantly reduce the data volume and rates transmitted to Earth.

During recent years, considerable effort has been devoted to the development of a digital radar image-processing capability. Unfortunately, results to date indicate that the digital data processing required to produce correlated radar images onboard a spacecraft or small aircraft is prohibitive based upon cost, complexity, power, size, and weight considerations. Since only limited data reduction, by means of presumming and time expansion, can be accomplished with the uncorrelated radar echo data, proposed radar mission requirements to date have implied the need for reliable high-speed and high-capacity tape recorders for storage and have imposed potentially severe requirements upon telecommunications link and ground data-handling capabilities.

The recent innovation of the charge-coupled device (CCD) transversal filter concept offers the potential for considerable simplification of the complicated digital implementation of convolution. A CCD transversal filter of length $N$ provides $N$ stages of analog storage while performing $N$ analog signal-by-weighting coefficient multiplications each clock period. Since the powerful computational equivalency of a CCD transversal filter significantly alleviates the constraints associated with digital processing, a CCD SAR image processor offers a potentially attractive answer to the real-time onboard SAR signal-processing problem.

## II. SAR Processing Principles

### The Synthetic Aperture

The concept of a synthetic aperture is illustrated in Fig. 1. Referring to Fig. 1, the term aperture refers to the size of the antenna. A larger antenna provides reduced beamwidth and higher azimuthal resolution, i.e.,

$$\delta_{az} = BR \tag{1}$$

$$B = \lambda/D \tag{2}$$

$$\delta_{az} = R\lambda/D \tag{3}$$

where $\delta_{az}$ = azimuth resolution, $B$ = beamwidth, $R$ = range, $D$ = antenna length, and $\lambda$ = wavelength. The physical size of a real-aperture antenna normally becomes too large to achieve an azimuth resolution comparable to the range resolution available from typical radar bandwidths. The process wherein a small antenna is used to simulate a large antenna in order to achieve a practical azimuth resolution is termed synthetic aperature. Synthetic-aperture radar (SAR) is based upon the fact that there is no difference between a large-aperature antenna and a small antenna that successively occupies all of the positions simultaneously occupied by the larger antenna, provided the data are successively collected, stored, and subsequently combined to simulate the larger antenna.

### Radar Data Acquisition

The basic process involved in acquiring SAR data is illustrated in Fig. 2. Repetitive energy pulses are transmitted to the surface to be imaged. The transmitted pulse normally has a known signature, such as a linear FM sweep or chirp. The resulting echo-return pulse is divided into $N$ range bins, where $N$ is a function of the desired resolution. A resulting set of $N$ range bins for a given azimuth position is called a range line. For each subsequent transmitted pulse, a new range line is generated. Since the radar physically moves in the time interval between transmitted pulses, each range line will be at a different azimuthal position. A number of range lines, corresponding to the number of pulse repetition frequency (PRF) echo returns required to synthetically simulate the desired real-aperture antenna, must be stored. The resulting matrix consists of rows that contain different time delays or ranges and columns that provide azimuthal information for a given range.

The information required to produce a single image element, from the matrix of Fig. 2, is dispersed throughout

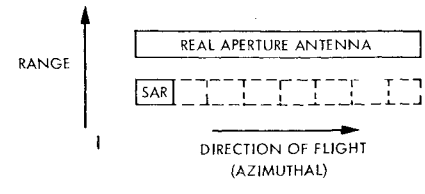


**Fig. 1 The synthetic aperture.**

Received Sept. 30, 1976; presented as Paper 76-967 at the AIAA Systems Design Driven by Sensors Conference, Pasadena, Calif., Oct. 18-20, 1976; revision received Sept. 9, 1977. 

Index categories: Aerospace Technology Utilization; Data Sensing, Presentation, and Transmission; Sensor Systems.

*Member of Technical Staff.

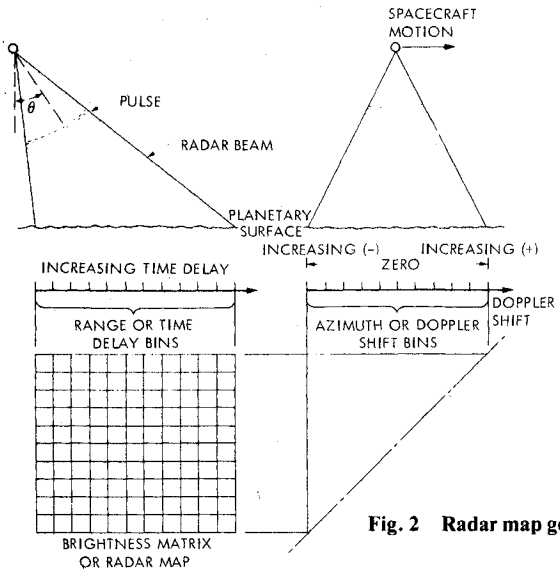


Fig. 2 Radar map generation.

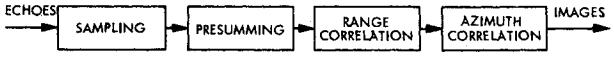


Fig. 3 SAR processing functions.

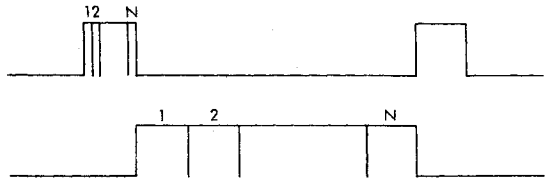


Fig. 4 Sampling and time expansion.

the matrix. In the time domain, correlation must be accomplished in both the range and azimuth dimensions in order to convert the dispersed echo data into images. The primary processing functions employed to convert echoes into image elements are defined in Fig. 3.

### Sampling

The sampling function of Fig. 3 is illustrated in Fig. 4. Basically, the pulse amplitudes are sampled at greater than Nyquist rate during the echo pulse duration and stored. The stored samples are then read out over the remaining pulse repetition interval (PRI), resulting in time expansion. The result is a data-rate reduction proportional to the echo pulse duty cycle.

### Presumming

The rationale associated with presumming is simplistically illustrated in Fig. 5. For SAR applications, the PRF is such that the azimuth resolution frequently exceeds the range resolution. On the assumption that the azimuth resolution does not have to be greater than that in range, echo pulses may be presummed (range bin 1 added to range bin 1, range bin 2 added to range bin 2, etc., over successive echo pulses). If the azimuth resolution were 6.25 m, then presumming every four pulses into one composite pulse would provide a resolution of 25 m. The result would be a data-rate reduction of 4. It should be noted that the presumming function of Fig. 5 is not practically accomplished by direct summation, but must be achieved by means of filtering to adequately reduce the aliasing effects.

### Range Correlation

The range-correlation function is illustrated in Fig. 6. In referring to Fig. 6, note that the correlation of an incoming

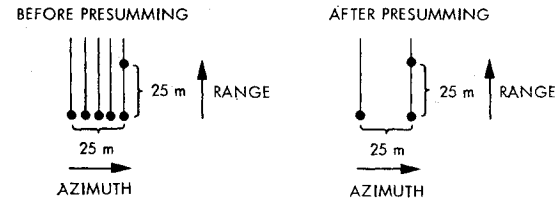


Fig. 5 Presumming.

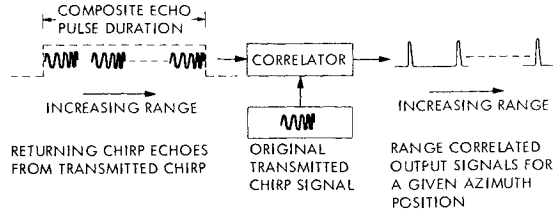


Fig. 6 Range correlation.

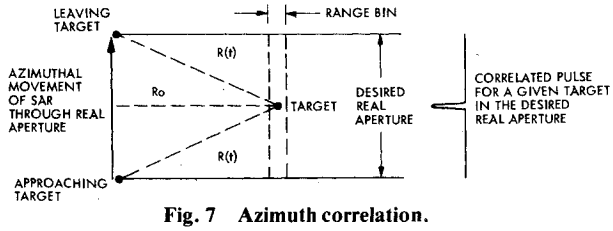


Fig. 7 Azimuth correlation.

chirp echo signal from a given target with a replica of the transmitted chirp signal results in a compressed pulse having a pulse width corresponding to the range resolution and a position in range corresponding to that of the actual target. The correlated chirp pulse width is inversely proportional to the transmitted chirp bandwidth, i.e.,

$$PW \sim 1/BW \tag{4}$$

Large bandwidths yielding high resolution can be accommodated because pulse compression (correlation) techniques allow the signal bandwidth to be expanded with negligible sensitivity loss.

### Azimuth Correlation

The azimuth-correlation function is described in Fig. 7. Referring to Fig. 7, signals from a given target will be received during passage of the SAR through the desired real aperture. Due to the Doppler effect, the carrier return from the target will be frequency modulated during the SAR passage through the desired real aperture. This FM is treated as a chirp function and is assumed to be a part of the input signal to the azimuth filter corresponding to the range bin in which the designated target lies. Correlation of this input signal with the expected Doppler chirp function across all azimuthal target positions relative to the SAR in the desired real aperture yields a compressed pulse having a pulse width corresponding to the azimuth resolution and a position in azimuth corresponding to that of the actual target. A larger number of correlation points (i.e., a longer correlation time) simulates a larger real aperture and therefore provides a narrower pulse width and improved azimuth resolution.

### *I* and *Q* Processing

Throughout the image-processing steps, it is desirable to preserve both amplitude and phase. This is best accomplished by *I* and *Q* channel processing as illustrated in Fig. 8. Echo-returns from a given target are vectors that vary in amplitude and phase with time. To combine these successive echo returns, as required for azimuthal processing, they must be broken into their real (*I*) and quadrature (*Q*) components.

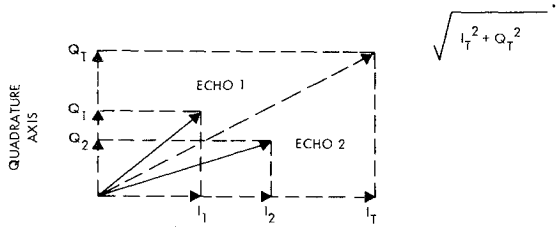


Fig. 8 *I* and *Q* signals.

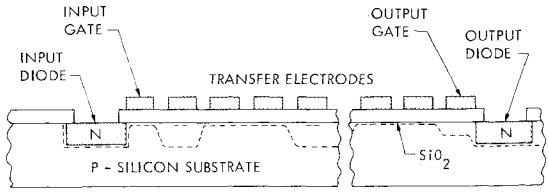


Fig. 9 CCD cross-section.

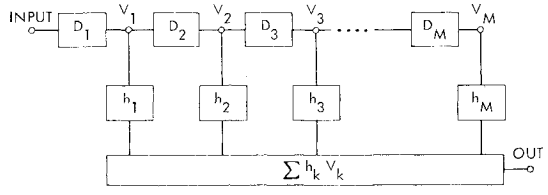


Fig. 10 CCD transversal filter.

The *I* signals for any echo are in phase so can be processed in the same correlator. In like manner, a separate correlator is required for the *Q* signals. Following *I* and *Q* correlation, the vector sum can be achieved by squaring and adding the *I* and *Q* voltage signals $(I^2+Q^2)$, yielding a sum proportional to the power.

## III. CCD Processing Techniques

### Transversal Filtering

A pictorial cross-section of a CCD is illustrated in Fig. 9. It functionally represents a device that stores packets of electrons or charge proportional to analog voltages. By controlling voltages to the transfer electrodes, these packets of charge may be transferred virtually intact from "potential well" to "potential well" through the device. The CCD, therefore, functions as an analog signal shift register. In Fig. 10, the stages of the shift register are depicted as $D_1$, $D_2$, etc. It is further noted that each of these outputs is nondestructively interrogated and multiplied by a factor $h_K$. These weighted outputs are then summed in a common summation network. This configuration, as a total entity, provides the transversal filtering function.

To illustrate how the cross-correlation function is achieved, assume that weighting $h_1$ through $h_m$ is that of the originally transmitted reference function. Furthermore, assume that each sample of the sampled radar reflection data is shifted through stages $D_1$ through $D_M$ of the filter. Once the register is filled, for each radar data sample shifted into the register a complete correlation of all $M$ points in the register with the reference function is automatically accomplished and a correlated output produced. The cross-correlation function is therefore achieved by nothing more than shifting the radar return data through a shift register.

Where the weighting function does not have to be programmable, i.e., when it is fixed and known, an extremely simple means of CCD fixed-tap electrode weighting can be achieved. The weighting function can be anything desired (chirp, PN, etc.) and is implemented by an electrode etching process. A different weighting function can be implemented during manufacture by simply using a different mask during the etching process.

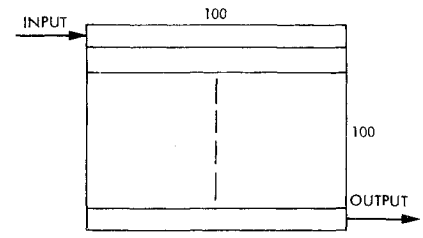


Fig. 11 CCD SPS memory plane.

### Memory

For memory applications where a very long delay line is functionally required, CCD serial-parallel-serial (SPS) techniques are especially attractive. For example, a typical SPS memory plane organization to accommodate 10,000 samples on a single chip is shown in Fig. 11. Referring to Fig. 11, the data are read into the memory plane in series and transferred in groups of 100 samples through the memory plane in parallel. If 100 such groups are accommodated, the storage capacity will be 10,000 samples. Just as the data are clocked serially into the memory, they are also read out in serial form from the last 100-sample group. As the last sample in the last 100-sample group location is read out, all 100-sample groups are shifted in parallel through the memory plane one position so that the last 100-sample group location is again filled. Serial readout can therefore be continued on an uninterrupted basis.

Several points concerning the CCD SPS memory organization are worthy of note. It is truly a first-in-first-out organization. The first sample in will be the first sample out, the second sample in will be the second sample out, etc. In other words, the SPS array is functionally the same as a long serial shift register. However, compared to a long serial shift register, each data sample of information sees more than an order of magnitude reduction in transfers through the memory. For instance, in Fig. 11, each data sample will only transfer through 200 stages between input and output as opposed to 10,000. This greatly simplifies charge transfer considerations, thereby making high-density analog storage practical.

### Fourier Transform

CCD technology may be used to accomplish the discrete Fourier transform (DFT). One application of the CCD DFT would be to achieve programmable transversal filtering. Instead of performing the filtering by convolution in the time domain (as illustrated in Fig. 10), it would be accomplished in the frequency domain. The concept is based upon the fact that convolution in the time domain

$$y = x * h \tag{5}$$

is exactly equivalent to multiplication in the transform domain

$$y = X \cdot H \tag{6}$$

Therefore, convolution could be achieved as illustrated in Fig. 12a by: 1) performing the DFT using the chirp-Z transform (CZT) algorithm, 2) multiplying by the transform of the desired impulse response, and 3) performing the inverse DFT ($DFT^{-1}$). Implementation of the DFT using the CZT results in the block diagram of Fig. 12b. Since two of the multiplication operations of Fig. 12b cancel, the block diagram of Fig. 12b could be replaced with the simplified block diagram of Fig. 12c. From an implementation standpoint, the CZT and $CZT^{-1}$ functions of Fig. 12c can be achieved by using CCD fixed-tap weighted filter chips. In other words, programmability can be achieved using CCD fixed-tap weighted filters by working in the frequency domain.

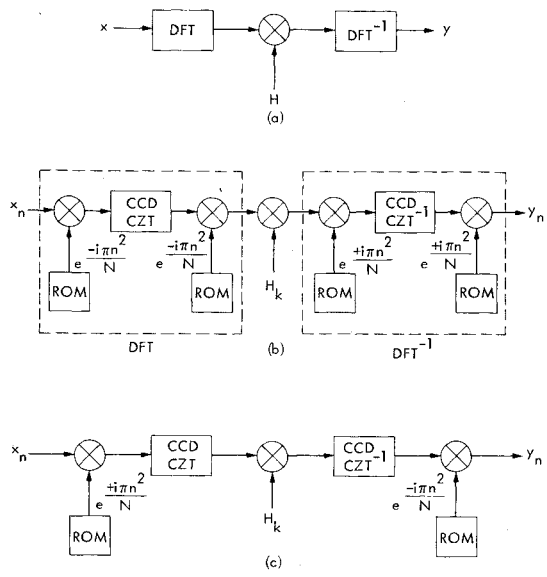


Fig. 12 CCD programmable transversal filter.

## IV. CCD Processor Architecture

### Sampler

A block diagram of a typical CCD SAR time-domain processor design architecture is illustrated in Fig. 13. The sampling function includes an input switch which samples video from the radar receiver and distributes the analog voltage samples into $N$ CCD storage registers. The samples are distributed to several registers in order to reduce the input data rate to any one CCD register. For example, if the input sampling rate were 25 mega-samples per second (Msps), and there were five registers, the maximum input rate to any one register would be 5 Msps. The sampling and storage operation is accomplished in real time during the echo pulse duration. Following storage in the registers, the samples are read out over the remainder of the pulse repetition interval (PRI) providing an effective time expansion. By using two such sampler units for which the input is alternated each PRI (during each PRI one is storing and the other reading out), the maximum possible time expansion can be achieved since readout occurs over the entire PRI.

### Presummer

A three-pole CCD recursive filter configuration is used to provide the presumming function for the system design of Fig. 13. As noted in Fig. 13, CCD registers are used as delay elements. Each register stores exactly one range line so that the range bins from preceding pulses are weighted and combined with corresponding bins from subsequent pulses. Where geometric corrections in the azimuthal direction are required for range migration, Doppler centroid shift, etc., such corrections would probably have to be made prior to presum filtering.

### Range Correlator

Assuming the reference function is fixed, the range correlation function of Fig. 13 could be accomplished by a fixed-tap weighted transversal filter. A typical implementation would include four transversal filters on a single chip to accommodate the sin and cos components for both the $I$ and $Q$ signals.

### Azimuth Correlator

Referring to Fig. 13, the first step in achieving the azimuth correlation function is accomplished by reading correlated range lines into a memory. Range bins are then read from the memory into a transversal filter wherein image elements are produced. Because of variations in the Doppler chirp function for typical flight applications, it is desirable that the correlation function be programmable. Furthermore, geometric corrections may also have to be applied to the data prior to correlation to compensate for range migration effects.

A potentially attractive architecture for the azimuth correlator, to provide both correlation function programmability and range migration correction capability, is illustrated in Fig. 14. Referring to Fig. 14, incoming samples are shifted into a serial-to-parallel converter and transferred to a memory chip capable of storing one range line. The memory organization consists of $N$ such chips cascaded to

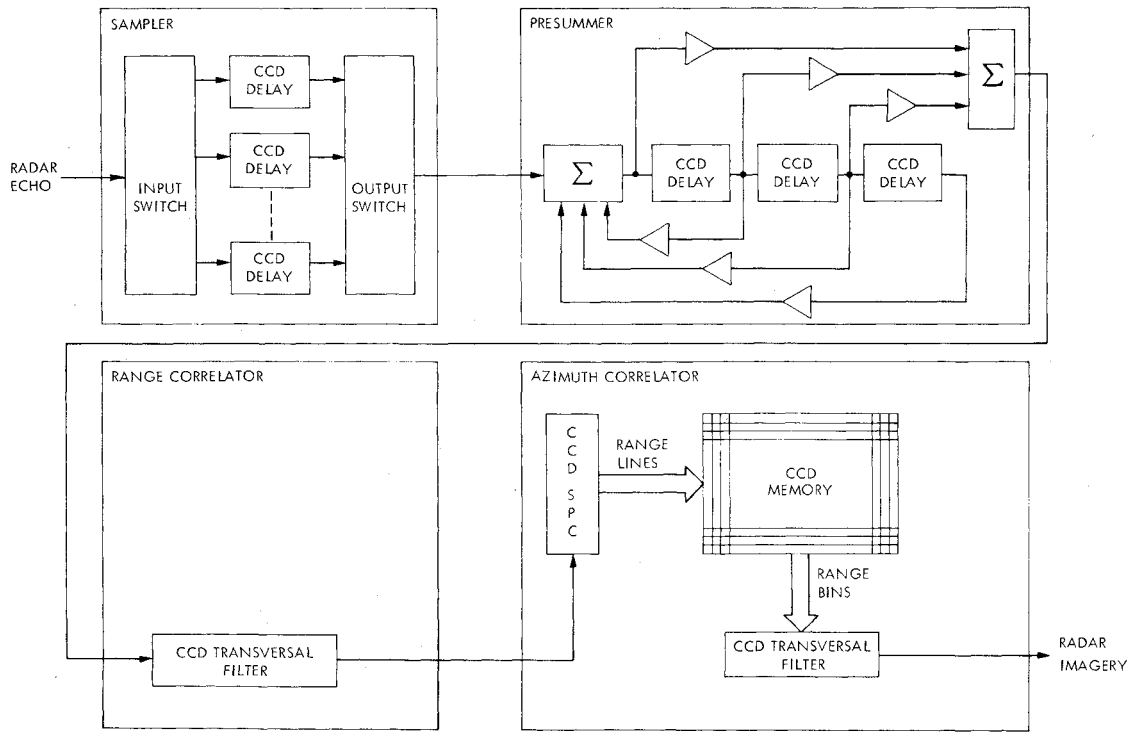


Fig. 13 Typical CCD SAR proccessing design.

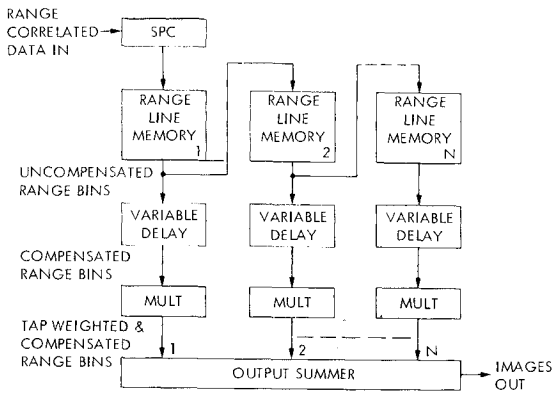


**Fig. 14 Time-domain azimuth correlator architecture.**

store sequential range lines. Enough range lines are stored to correspond to the number of points required to correlate over the real aperture in the azimuth dimension. It is further noted from Fig. 14 that the last stage of each range-line memory chip is separated from the last stage of the preceding and subsequent range-line memory chips by exactly one range line. The outputs of the last stages, taken together, therefore form a complete and unique range bin in the azimuthal dimension at any given time. For each unique sample from a range line that is shifted into memory, every sample moves one stage through the entire cascaded memory array. The net result is that an entirely new set of samples occurs at the output stages of the range-line memory chips corresponding to a new azimuthal range bin. Therefore, the need for a high-speed random-access memory is eliminated. The desired azimuthal range bins to be corrected and subsequently correlated are automatically read out of the memory in parallel on a range-line sample-by-sample basis. The readout rate cannot be greater than the range-line sample rate resulting in the most efficient transfer of data possible.

The next step in the azimuthal processing operation is to perform range migration compensation on the range bins. This is precisely accomplished, using the variable delay function of Fig. 14, with no need for interpolation or other methods of approximation. The variable delay is actually accomplished as shown in Fig. 15. The output of the last stage of each range-line memory chip is read into an $N$-stage register where $N$ is the maximum number of bins over which migration occurs. In effect, the $N$-stage registers as a group are storing parallel uncompensated azimuthal range bins. Compensation is accomplished by selecting information from any location within each register to form the desired range bin for correlation. The net effect is the same as sliding every range line in a matrix in either direction through range bins until the desired samples are in the range bin to be correlated. To avoid interpolation and achieve a precise correction, it is necessary to reconstruct the curve within the range bin and effectively resample on the curve at the correct location. This can be accomplished by using a sin $x/x$ algorithm. If the range-correlator output in the form of range-line samples (which is exactly what is in each $N$-stage register of Fig. 15) is convolved with a digitally sampled $\sin x/x$ function, the original range-correlated signal will be reproduced. However, by shifting the phase of the $\sin x/x$ signal such that it is sampled at different points, the same range-correlated signal will be reproduced following convolution, only it will also be sampled at different points corresponding to the phase shift of the $\sin x/x$ signal. As such, a precise resampling within a range bin may be accomplished to accommodate the desired correction curve exactly.

As noted from Fig. 15, range-correction logic positions the $\sin x/x$ function in each register of each channel at the precise location to accommodate the correction curve. The reproduced signal following convolution will be the range-line element from the desired location in the $N$-stage register properly resampled to precisely correspond to the range-migration correction curve. The net result will be that for every range-line sample transferred into the memory, a fully compensated azimuthal range bin automatically falls out of the correction stages.

Each range-bin element of a compensated range bin is then weighted using a conventional multiplier. The outputs of each

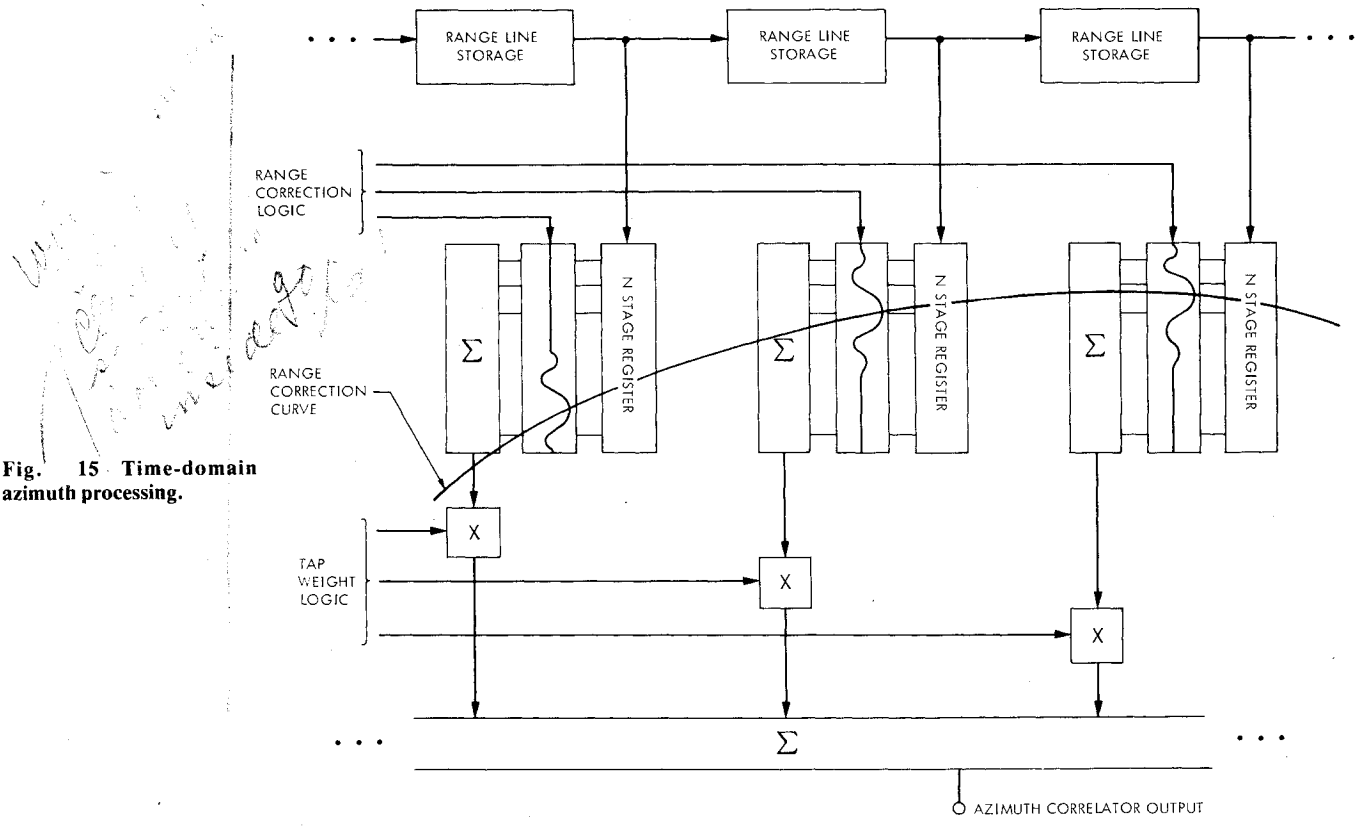


**Fig. 15 Time-domain azimuth processing.**

multiplier are then summed to form an image element for each range-bin correlation. The tap weighting for each range-bin element is fully programmable and could be updated from a microprocessor to accommodate orbital parameter changes in altitude, velocity, slant range, etc.

## V. CCD Aircraft Processor Development

### Flight Design

Following successful development and evaluation of a CCD laboratory breadboard processor, the design of a complete aircraft SAR image processor was undertaken and completed.[1-4] This processor was designed to be compatible with the JPL L-band radar already in existence on the NASA Convair 990 (CV-990) aircraft.

A block diagram of the aircraft SAR processor system design is provided in Fig. 16. As noted from Fig. 16, the aircraft processor is actually a hybrid system using both CCD and digital techniques. It uses analog CCD technology for the sampler, range correlator filters, and azimuth correlator filters. The presum filter and the azimuth correlator memory designs are implemented digitally to minimize development costs. Also, for cost reasons, the aircraft processor design is limited in performance capability to a 5 km swath width, 25-m resolution, and single-look imagery. If this development is successful, modification to accommodate greater swath widths, higher resolution, and multiple looks should be practical.

The CCD sampler is designed to accommodate a system swath width of 4.935 km. The required video information is, therefore, contained in a time period of 20.52 $\mu$s. During this brief period of time, the received video is sampled 513 times at a rate of 25 MHz. These samples are temporarily stored in a 513-cell CCD register and shifted out during the remaining 980 $\mu$s of the radar PRI. In this manner, a time expansion (approximately 48) of the sampled video data is achieved, allowing the data to be recorded and/or processed at a much lower rate.

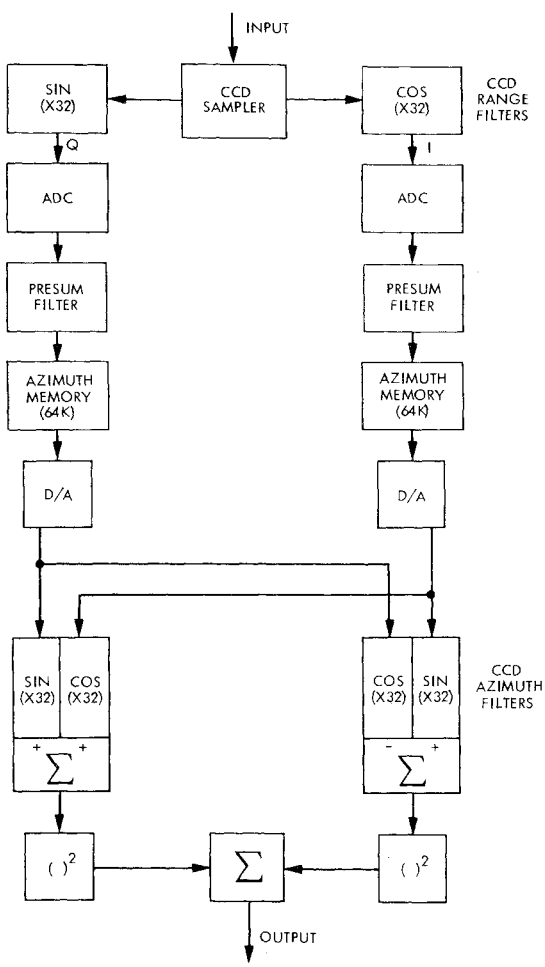


**Fig. 16 CCD aircraft SAR processor block diagram.**

The input sampler also receives a PRF synchronization pulse as well as a 5-MHz signal from the L-band radar. These signals are used to clock the input sampler so that the sampled radar-return video will be sampled at the same time delay after each radar PRF synchronization pulse.

Range correlation of the sampled radar video is performed by 32-cell CCD transversal filters. Processing of the data into pseudo-real and imaginary components ($I$ and $Q$) is effected by processing the sampled return through both a cosine filter and a sine filter, which are matched to the radar chirp, and then selecting alternate filtered output samples. This technique of taking alternate samples reduces the data rate, in range, by a factor of two. After range correlation, the $I$ and $Q$ signals are converted by an analog-to-digital converter (A/D) into a digital format.

At this point, presum filtering in azimuth (factor of 8) of the range-correlated data is performed to lower the data rate. Presum filtering also allows the subsequent azimuth correlation to be performed with a minimum azimuth correlator length and provides attenuation to the alias interference generated in the sampling process.

Azimuth correlation, like range correlation, is performed by 32-cell CCD filters. In the interest of economy, only one set of CCD filters is used for the $I$ channel and one for the $Q$ channel. These filters are used to process an entire 240-sample radar return by temporarily storing the data in a 64-K MOS memory. The memory contents are read out and digital-to-analog converted (D/A) prior to being processed by the CCD azimuth filter. Since the entire memory contents are read out in one PRI, the resulting azimuth processing is equivalent to the use of 240 separate parallel CCD filters for both the $I$ channel and the $Q$ channel. After azimuth processing, the $I$ and $Q$ channel outputs are squared and then summed to produce the final image output.

### Flight Testing

During flight, a digital tape recorder is used to record both the raw radar-return video at the output of the sampler and the processed images at the output of the processor. The recorder selected for use is a Sangamo Sabre III high-speed digital recorder. This recorder has an 11-bit parallel recording capability and two FM record channels. It uses 1-in. tape and records at 60 in./s. Playback is accomplished at either 60 in./s or 1 7/8 in./s. Special interface equipment allows tape dumps (at 1 7/8 in./s) to be made onto 9-track computer-compatible tapes for use in non-real-time computer processing of the data. The processed output of the processor is recorded on one of the unused channels.

The output of the CCD aircraft SAR image processor is displayed on a 9-in. TV monitor. This output is A/D-converted so that storage of an entire frame of data can be effected digitally. A scan converter is used either to hold and display the same image or to provide a rolling display during flight. The real-time display can also be used to display the data processed and recorded during flight at some later time for subsequent evaluation in the laboratory.

## Acknowledgment

This paper presents the results of one phase of research carried out by the Jet Propulsion Laboratory, California Institute of Technology, under contract with Texas Instruments, Dallas, Texas. This work has been sponsored by the National Aeronautics and Space Administration, code numbers 161-06-03 (EODAP) and 638-40-05 (AAFE), under Contract NAS 7-100.

## References

[1] "Radar Image-Processor Development Feasibility Study," Texas Instruments, Dallas, Tex., JPL Contract 953954, Final Rept., Dec. 1974.

[2] "Radar Image-Processor Development Program," Texas Instruments, Dallas, Tex., JPL Contract 954087, Final Rept., Dec. 1975.

[3] Bailey, W., et al., "CCD Application to Synthetic Aperture Radar," *Proceedings of CCD Applications Conference,* San Diego, Oct. 1975, pp. 301-308.

[4] Bailey, W., et al., "A Synthetic Aperture Processor Using CCD Signal Processing Techniques," *Proceedings of NASA/JPL Conference on CCD Technology and Applications*, Washington, D. C., Nov./Dec. 1976, pp. 21-7.